FIRST STEPS TOWARDS THE DESIGN OF AN ACTIVE PITCH LINK LOADS REDUCTION SYSTEM USING NOVEL CONTROL TECHNIQUES

Mark Voskuijl,
Flight Science and Technology
The University of Liverpool
Liverpool, U.K.
Mark.Voskuijl@liverpool.ac.uk

Dr. D. J. Walker
Flight Science and Technology
The University of Liverpool
Liverpool, U.K.
D.j.walker@liverpool.ac.uk

Dr. B. Manimala
Flight Science and Technology
The University of Liverpool
Liverpool, U.K.
Binoy@liverpool.ac.uk

Dr. R. Kureemun
Flight Science and Technology
The University of Liverpool
Liverpool, U.K.
R.kureemun@liverpool.ac.uk

Abstract

Several research studies have indicated that pitch link loads for various rotorcraft types can reach high or even unacceptable values, both in steady state and manoeuvring flight. This is especially the case for high-speed aggressive manoeuvres. An investigation into the nature of the pitch link loads for the FLIGHTLAB Generic Rotorcraft has been conducted and the model is expanded with a dynamic stall component and a flexible pitch link component to improve its fidelity. The investigation also shows that steady state pitch link loads are large for high-speed flight and they are amplified significantly whilst executing aggressive manoeuvres at high-speed flight. An active controller is designed to alleviate these loads for longitudinal manoeuvres at high- speed. A new structural load severity scale is defined in this paper to evaluate structural loads in combination with the load quickness parameter. The pitch link loads of the non-linear FLIGHTLAB Generic Rotorcraft simulation model can be reduced effectively with the controller but the agility of the aircraft is consequently reduced. The structural load metrics are shown to be effective in evaluating the controller.

List of Symbols and Abbreviations

a_{1s}	Lateral cyclic pitch angle [rad]
a_{ph}	Pitch horn arm length [ft]
b_{1s}	Longitudinal cyclic pitch angle [rad]
c	Chord [ft]
$C_{pitchlink}$	Damping of the pitch link [lbf-s/ft]
C_m	Moment coefficient [-]
D	Damage [-]
F_{pl}	Pitch Link Load [lbf]
F_{pk}	Peak oscillatory load [lbf]
F_{ss}	Steady state oscillatory load [lbf]
K	Controller matrices
k	Reduced frequency [-]
$K_{pitchlink}$	Pitch link stiffness [lbf/ft]
k_θ	Control system stiffness [ft-lbf/rad]
M	Mach number [-]
M_x	Pitching moment at the blade root [lbf-ft]
$M_{x,Coleman}$	Coleman Transformation of the pitch link load [ft-lbf]
N	Number of cycles [-]
p	Roll rate [rad/s]
P	Plant matrices
q	Pitch rate [rad/s]
Q_θ	Attitude quickness [1/sec]
Q_γ	Agility quickness [1/sec]
Q_l	Load quickness [lbf/deg]
r	Yaw rate [rad/s]
r	Non-dimensional rotor radius [-]
R	Rotor radius [ft]
S_a	Stress amplitude [lbf / ft^2]
S_m	Mean stress [lbf / ft^2]
S_{min}	Minimum stress [lbf / ft^2]
S_{max}	Maximum stress [lbf / ft^2]
t_{MTE}	Time duration of mission task element [s]
u	Vector of control variables
v	Vector of measured variables
V	Flight speed [ft/s], [kts]
w	Vector of exogenous variables (reference, disturbance)
x_a	Lateral stick position [%]

Paper presented at the 31st European Rotorcraft Forum, 13-15 September 2005, Florence, Italy

x_b	Longitudinal stick position [%]
x_c	Collective stick position [%]
x_p	Pedal position [%]
z	vector of 'error' signals
Δ	Elongation of the Pitch Link [ft]
ϕ	Roll attitude [rad]
θ	Pitch attitude [rad]
θ	Pitch angle of the blade [rad]
θ_0	Collective pitch angle [rad]
$\theta_{0,tr}$	Tail rotor collective pitch angle [rad]
ω	Frequency [rad/s]
Ω	Rotor rotational speed [rad/s]
ψ	Yaw attitude [rad]
ψ	Azimuth angle [rad]
ACAH	Attitude Command Attitude hold
ASRA	Advanced Systems Research Aircraft
EDLIN	Equations Differentielles Lineaires
FAR	Federal Aviation Regulations
JAR	Joint Aviation Requirements
FEP	Flight Envelope Protection
FGR	Flightlab Generic Rotorcraft
HELI-ACT	Helicopter Active Control Technology
HQ	Handling Qualities
IBC	Individual Blade Coordinates
LAF	Load Amplification Factor
MBC	Multi Blade Coordinates
MTE	Mission Task Element
NACA	National Advisory Committee for Aeronautics
NRC	National Research Council
PI	Proportional and integral
SCAS	Stability and Control Augmentation System
SLA	Structural Load Alleviation
UoL	University of Liverpool

1. Introduction

Several research studies [Ref 1-5] have indicated that pitch link loads for various rotorcraft types can reach high or unacceptable values, both in steady state and manoeuvring flight. This is especially the case for high-speed aggressive manoeuvres. Action should conceivably be undertaken to protect the pitch link from high loads. The aim of this paper is to investigate the use of active control and to present the design of an active control system that will alleviate and/or protect the pitch link load depending on the nature of the load. There are hardly any metrics available to evaluate the structural loads objectively. The second aim of this paper is therefore the definition of new load metrics.

This work is performed within the HELI-ACT (Helicopter Active Control Technology) project, which involves collaboration between the University of Liverpool (UoL) and the National Research Council (NRC) of Canada, European research centres and Industry. Use is made of a sophisticated six-axis Flight Simulator at the University of Liverpool, and a Bell 412 fly-by-wire research helicopter, operated by the NRC. Several FLIGHTLAB rotorcraft simulation models are available for both off-line and real-time use in the Flight Simulator. One model is of NRC's Advanced Systems Research Aircraft (ASRA), recently developed within the HELI-ACT project [Ref 6].

This project has two strands, one related to model development, the other to active control for handling qualities, flight envelope protection and structural load alleviation (HQ, FEP and SLA). The Flightlab Generic Rotorcraft (FGR) simulation model is used in this paper as research tool. The FGR is very similar to the UH-60A Black Hawk helicopter.

The design of an active control system for pitch link loads requires a good understanding of the nature of the loads acting on the pitch link. This understanding can be acquired through actual flight tests or by simulations. Use is being made of the FGR simulation model in the absence of flight test data. Flight test data from the ASRA will be used when it becomes available. The FGR is a helicopter with an articulated rotor. This model of course has to have the right detail to provide a reasonably accurate prediction of the pitch link loads. The pitch link loads are very closely related to the blade pitching moment at the blade root. This pitching moment is the result of the air loads and the blade dynamics. This raises a number of questions. What kind of wake model has to be used? Does blade (torsional) flexibility have to be modelled? Is it required to model control system stiffness? What kind of air loads modelling is necessary? The answers to these questions can be found in literature, e.g. Ref. 7, which describes an extensive study of the calculation of pitch link loads. One of the conclusions of the study was that the effect of blade torsional stiffness on overall pitch

link load response is insignificant. The question whether this is true or not will be addressed in the continuing HELI-ACT project. For now, blade flexibility will not be modelled. The same reference indicates that a proper representation of control system stiffness is required for the prediction of pitch link loads. The FGR model has rigid blades, a 3-state dynamic inflow model, quasi-steady air loads and control system stiffness is not modelled. Based upon the conclusions from reference 7 it was decided to extend the FGR model with a flexible pitch link model. The rotor blades operate in an unsteady environment close to the stall limits for high-speed aggressive manoeuvres [Ref 8]. It is therefore decided also to extend the FGR model with a dynamic stall model. It was also decided not to use a free wake model. The reason for this is twofold. First of all, the influence of a free wake model is probably not that large at high-speed flight [Ref 9], while this is exactly the flight condition upon which this research study is focused. Secondly, this project will include real time piloted simulator trials in the future and it is not yet clear whether a free wake model can be made to run in real-time with the FLIGHTLAB model.

The structure of this paper is as follows. The next two sections will describe the implementation of the flexible pitch link model and the dynamic stall model. The impact on flight dynamics and structural loads due to both models will then be evaluated. The manoeuvre to be evaluated for which a first SLA system will be designed is a high-speed pull-up manoeuvre. The next paragraph examines the design of this SLA system, using a linearised model of the FGR. This controller is subsequently implemented in the non-linear model and tested offline. New load metrics are presented for the analysis. Finally conclusions and recommendations are drawn.

2. Modelling

2.1 Implementation of the pitch Link model

The pitch link was modelled as a linear spring and damper (Fig 1).

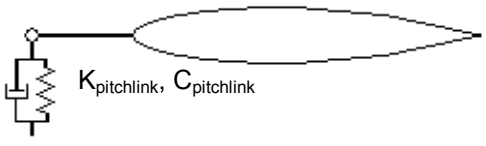

Figure 1: Pitch Link model

This essentially means that a torsional degree of freedom is added to the model. There is currently no accurate pitch link data available for the UH-60 Black Hawk (such as stiffness, damping and dimensions). However, the pitch link stiffness of the Sikorsky S-76 can be derived from the data in table 1 [Ref 10]:

Variable name	Variable	Value
Control system stiffness	k_θ	24000 [ft-lb/rad]
Pitch Horn Arm	a_{ph}	0.54 [ft]
Rotor Speed	Ω	30.7 [rad/s]

Table 1: Sikorsky S-76 Hub retention system data [Ref 10]

The equations needed to calculate the pitch link stiffness from this data are given in appendix A. It follows that the pitch link stiffness is equal to 82304 [lb/ft]. No information is available on the damping coefficient of the pitch link ($C_{pitchlink}$). The pitch link is assumed to have 1% critical damping, as an initial guess. It is not expected that this torsional degree of freedom will have a significant influence on the flight mechanics because the natural frequency is high compared to the rotor rotational frequency.

2.2 Implementation of the dynamic stall model

The pitch link loads are highly dependent on the blade pitching moment. The rotor blades themselves operate in a very unsteady dynamic environment, especially when manoeuvres are performed. It is known that the resulting aerodynamic force on a rotor blade operating in this unsteady environment is dependent on the frequency of the pitching motion, the plunging motion (blade flapping) and of the vertical translation (vertical gusts from rotor wake etc.). In the aero-elasticity literature it is shown that the so-called reduced frequency *k*, given by equation 1, is a key parameter in describing the unsteadiness of the flow field.

$$k = \frac{\omega c}{2V} \qquad (1)$$

According to [Ref 8], the flow is generally called unsteady whenever the reduced frequency is larger than 0.05. The reduced frequency is usually much larger than 0.05 whenever the pitching motion of a helicopter rotor blade is considered. In that case it can easily reach a value of about 0.2 (e.g. when

the torsional mode shape or inboard radial stations are considered). This means that unsteady aerodynamics should be modelled for the simulation of pitch link loads. As stated in the introduction, the pitch link loads become large for high-speed aggressive manoeuvres. Large portions of the rotor disk can then be subjected to stalled conditions and a phenomenon called dynamic stall can occur. Leishman [Ref 8] has defined dynamic stall as follows:

"Dynamic Stall will occur on any airfoil or lifting surface when it is subject to time-dependent pitching, plunging or vertical translation, or other type of non-steady motion that takes the effective angle of attack above its normal static stall angle. Under these circumstances, the physics of flow separation and the development of stall have been shown to be fundamentally different from the stall mechanism exhibited by the same airfoil under static (quasi-steady) conditions. Dynamic stall is in part, distinguished by a delay in the onset of flow separation to a higher angle of attack than would occur statically"

Dynamic stall has positive and negative effects. The main positive effect is better performance because higher lift is achieved on the rotor disk. One of the principal negative effects according to the literature is the increase of torsional loads on the blade. Little research has been done to determine the influence of dynamic stall on flight mechanics [Ref 11].

A review of the different dynamic stall models available today is given in reference 13. One model in particular is the ONERA EDLIN (Equations Differentielles Lineaires) model, described in references 12 and 14. This model has been linked to the FGR model and is used in this work. It uses a set of non-linear differential equations and describes the unsteady airfoil behaviour in both attached and unattached flow. A set of dynamic stall parameters is required for the dynamic stall model. These parameters can be determined via wind-tunnel experiments. The rotor blades of the FGR are modelled with a NACA 0012 aerofoil. The dynamic stall coefficients for this aerofoil are given in Ref 14.

The nature of the pitch link loads and the influence of the flexible pitch link model and dynamic stall model upon this load and upon the flight mechanics is described in the following 3 paragraphs.

3. Loads Analysis

3.1 Pitch link loads in steady state level forward flight

The pitch link loads are calculated in steady state level forward flight as a starting point. Figure 2 shows the pitch link load as a function of flight speed.

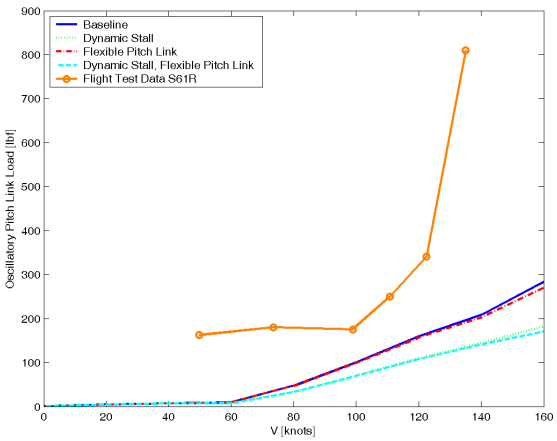

Figure 2: Oscillatory pitch link load as a function of flight speed

The oscillatory pitch link load, i.e. half of the peak-to-peak variation over one azimuth, is very low for flight speeds up to 60 knots and then starts to increase in a linear manner. This is the case for all four models. The models with dynamic stall however show a lower value. Flight test data for the Sikorsky S-61 helicopter [Ref 15], included in figure 2 as an example, shows the same trend as the simulation results. The oscillatory pitch link load is low until a certain flight speed and then increases significantly.

One must bear in mind that the S-61 is a different helicopter, so only the trend of the lines was expected to be similar. One important difference with the FGR is that the aerofoil of the S-61 is cambered. This is probably the cause of a significant constant oscillatory pitch link load at low speeds. The highest oscillatory pitch link loads for the FGR are encountered at the maximum speed considered, which is 160 knots. These are plotted in figure 3 on the next page as a function of rotor azimuth

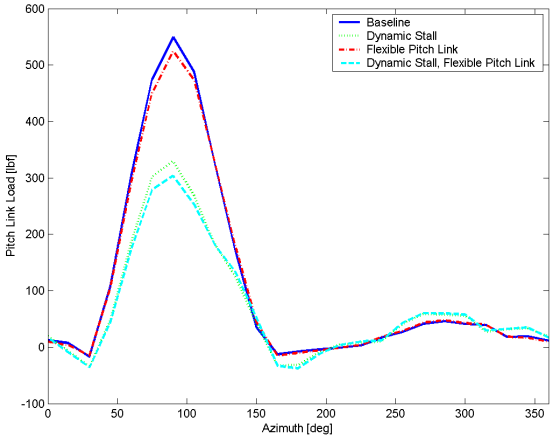

Figure 3: Pitch link load as a function of rotor azimuth in steady level flight at 160 knots

The pitch link load is approximately zero over a large portion of the rotor disk and increases at the advancing blade side. A large peak can be seen here for the four models considered in figure 3. The dynamic stall model predicts a peak value of the pitch link load that is about 40% less than the baseline model.

3.2 Impact of the pitch link model and dynamic stall model on flight mechanics

To investigate the effects of the flexible pitch link model and the dynamic stall model on the flight mechanics of the FGR, several offline simulations have been performed at 120 knots forward flight speed. Step inputs are applied in all control channels for four different models:

- Baseline
- Baseline + Dynamic Stall
- Baseline + Flexible Pitch Link
- Baseline + Dynamic Stall + Flexible Pitch Link

The baseline model is the FGR without SCAS (bare airframe). The SCAS is turned off because it might conceal the effects of the models on flight mechanics. Figures 4 -7 present the aircraft response for the offline simulations.

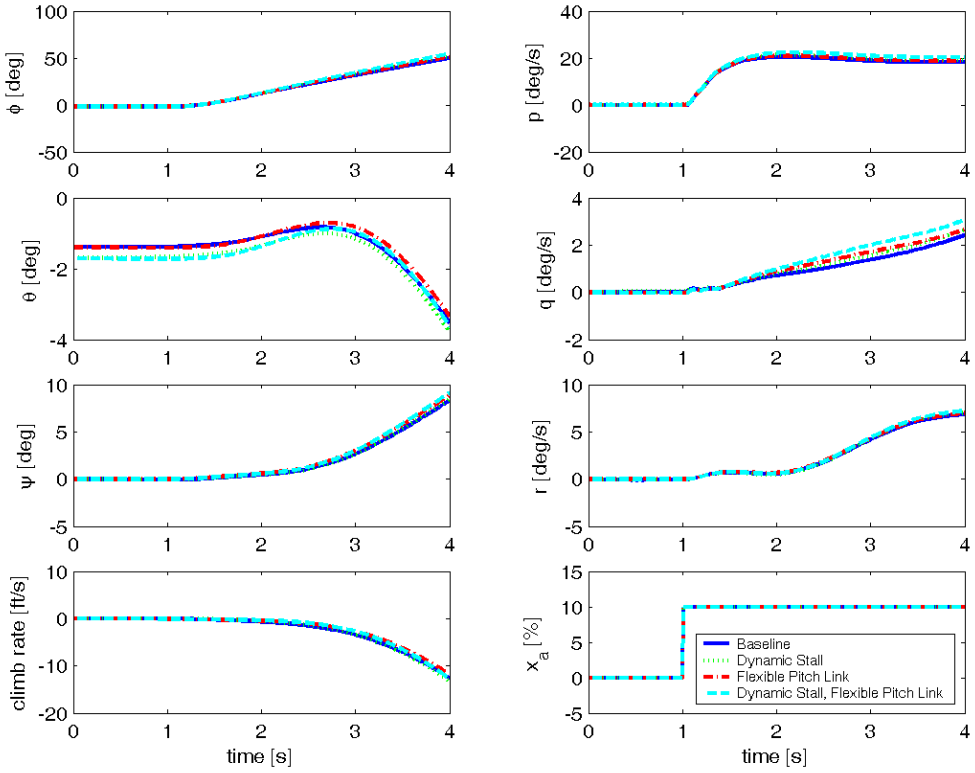

Figure 4: Lateral stick input at 120 knots, SCAS off

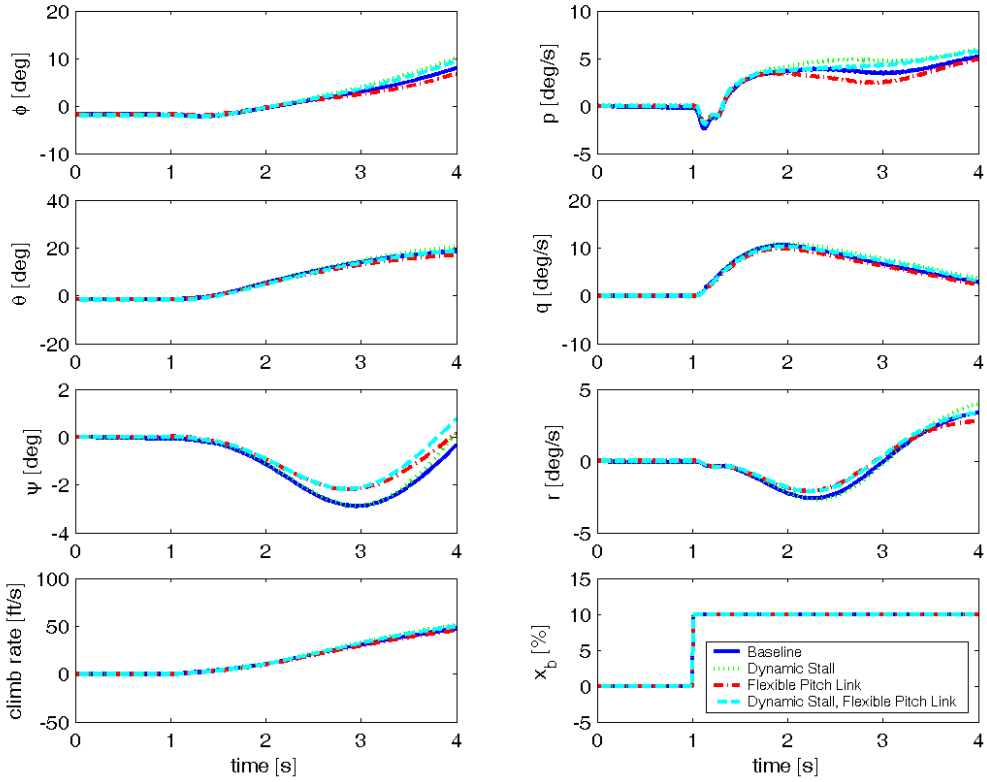

Figure 5: Longitudinal stick step input at 120 knots, SCAS off

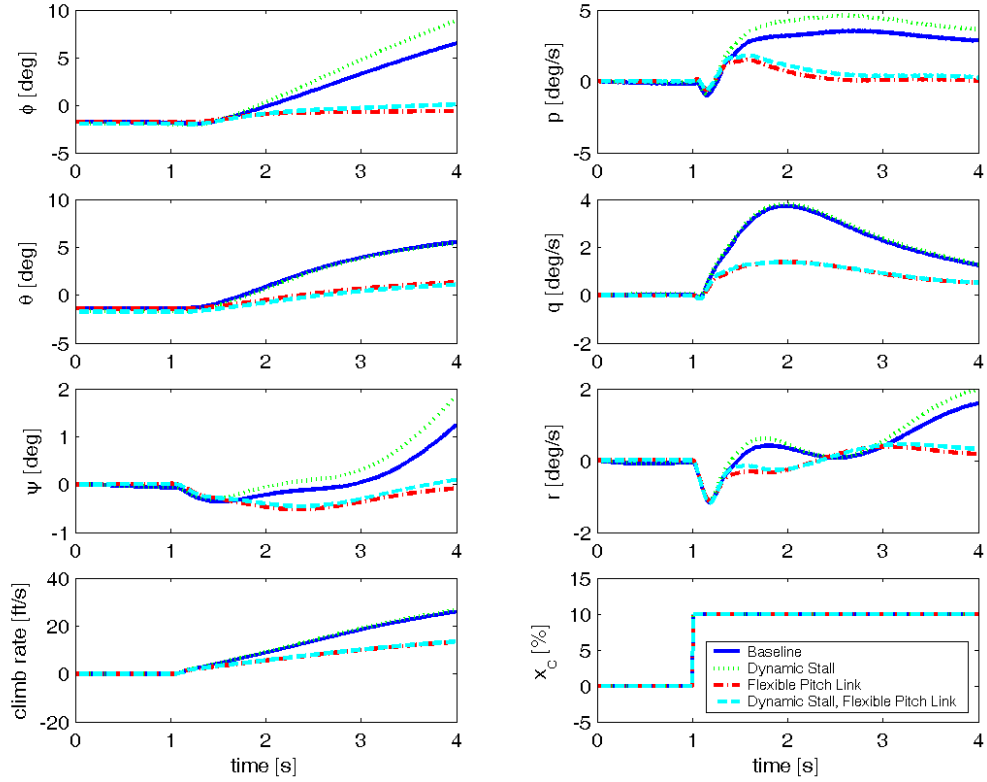

Figure 6: Collective stick step input at 120 knots, SCAS off

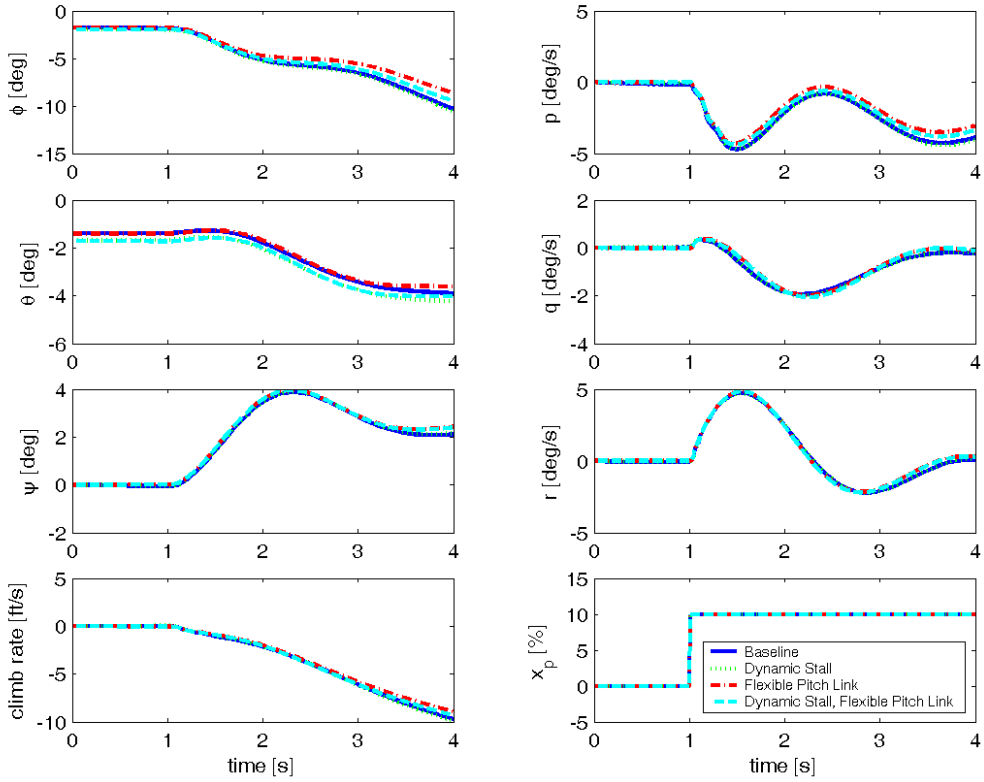

Figure 7: Pedal step input of 10% at hover 120 knots, SCAS off

The above figures suggest that the effect of dynamic stall on the aircraft attitudes, rates, flight path and other related variables is insignificant. It may be possible that its effect will become noticeable for more aggressive manoeuvres where large portions of the rotor disk are subject to stall. The flexible pitch link does not have a significant effect on flight mechanics either. The impact on the aircraft attitudes, rates, flight path and other related variables for lateral, longitudinal and pedal inputs due to the new torsional degree of freedom is within a couple of percent, as was expected. The flexible pitch link model does have a noticeable effect on the flight mechanics when collective inputs are considered. The initial response in the first second after applying the input is very much the same, but the achieved climb rate is reduced after the first second.

Responses at other flight speeds are very similar, i.e. the impact of dynamic stall and a flexible pitch link model on flight mechanics is very much the same as at 120 knots.

4. High speed control law

The main goal of this research is to design a pitch link SLA controller for pull up manoeuvres at high-speed flight. A pull-up is therefore performed with the four different models to evaluate the transient pitch link load behaviour (Fig. 8 on the next page).

The pull-up is executed by a simple longitudinal stick step input of approximately 20% full-scale deflection. The lateral states of the model are frozen so there is no off-axis response. This is done to keep the four manoeuvres very similar. The load factor encountered due to such an input is close to 2 g. The flight speed at the start of the manoeuvre is 120 knots. The structural envelope of the UH-60A [Ref 2] allows manoeuvres up to 3.5 g at this speed. So this manoeuvre is executed well within the structural flight envelope of the FGR. One can see that the transient behaviour of the pitch link load is similar for the four models. Dynamic stall causes a higher frequency content of the load. The flexible pitch link model is the cause of a larger transient load compared to the baseline value.

4.1 ACT system design for Loads reduction

It is the intention of the first preliminary SLA controller design merely to prove the feasibility of an SLA controller for the pitch link loads. The first investigations are primarily for longitudinal manoeuvres.

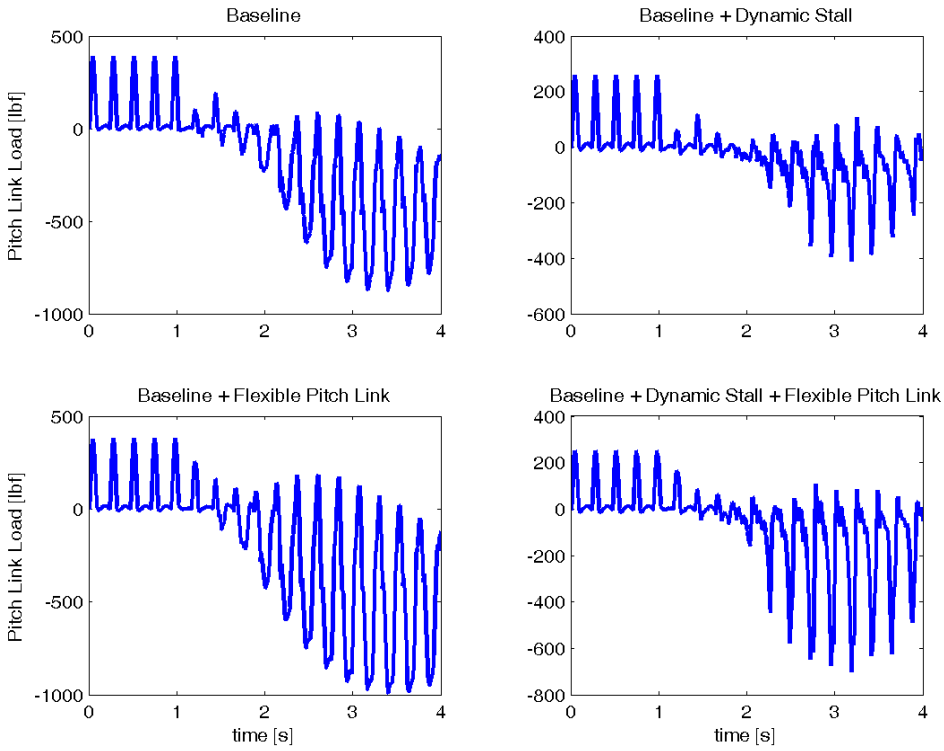

Figure 8: Transient pitch link loads for a 2 g pull – up manoeuvre at 120 knots

A linearised model of the FGR is required for control law design. Unfortunately, the oscillatory pitch link loads cannot be linearised in the usual manner because they are variables in the individual blade coordinates (IBC). A Coleman transformation is therefore used to represent the loads acting on the individual blades in multi blade coordinates (MBC) [Ref 16]. A 9-state linearised model of the FGR at 120 knots in trimmed level forward flight, with a pitch link load envelope ($M_{x,Coleman}$) as one of the outputs, is obtained from the baseline non-linear FGR model.

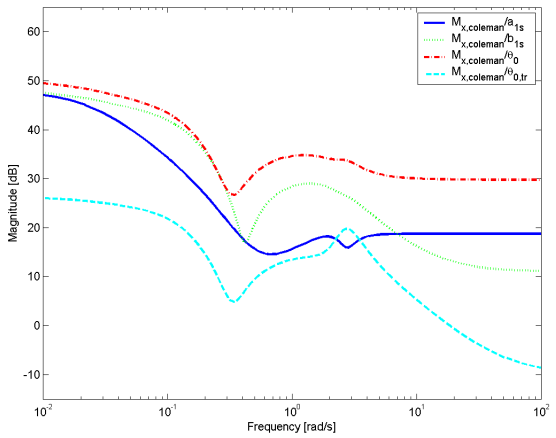

Figure 9: Open loop frequency response of pitch link load envelope ($M_{x,Coleman}$)

An open loop frequency response is performed to evaluate the influence of the different control inputs on the pitch link load envelope (Fig 9).

The open loop frequency response shows that the collective pitch angle has the largest effect on the load of all the control inputs. The controller is therefore designed to control collective pitch θ_0. The controller is synthesised using H_∞ optimisation. The variables selected as feedback signals for the controller are the longitudinal states: θ and q. The complete feedback control system is shown in Fig. 10.

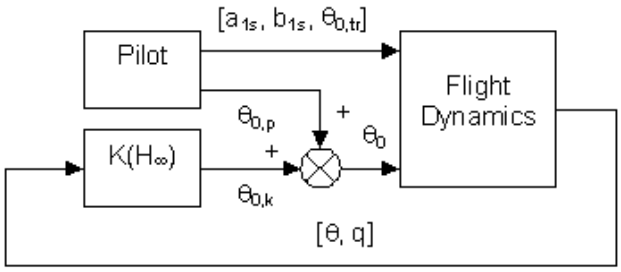

Figure 10: Basic feedback control systematic to alleviate pitch link loads in longitudinal manoeuvres

The controller matrices are derived with the MATLAB® algorithm *hinflmi* [Ref 17]. The

signals needed for the general control configuration (appendix B) are the following.

$$\vec{z} = \left[M_{x,Coleman} \right]$$
$$\vec{v} = \left[\theta \quad q \right]$$
$$\vec{w} = \left[0 \right]$$
$$\vec{u} = \left[\theta_0 \right]$$

H_∞ optimisation was used to synthesise a stabilizing controller transfer function K that minimized the energy-gain from w to z. Simple gains have been set on the measured variables to get an acceptable load reduction. The evaluation of the SLA controller is done in combination with a simple PI-controller for the pitch channel, providing pitch ACAH. The PI controller is used to obtain a similar response in pitch (i.e. overall manoeuvre) for both simulations.

The linearised pitch link loads are successfully reduced while the primary (pitch) response of the linearised FGR (Fig 11) is almost the same for the model with SLA and the model without SLA.

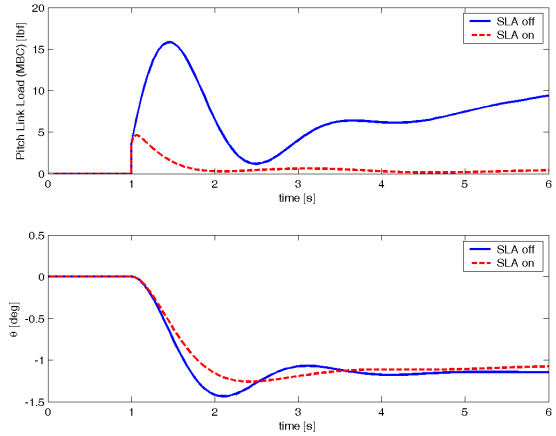

Figure 11: Reduction of load

The off-axis response was not fixed for the linear analysis. It changes slightly but it does not really change handling qualities. This controller was implemented in the baseline non-linear FGR model and it is evaluated in the next two paragraphs.

4.2 Definition of new structural load metrics

Rotorcraft structural components are subject to both static and dynamic loads. The maximum static load that a component has to be able to withstand is clearly defined in the Federal Aviation Regulations (FAR) and the Joint Aviation Requirements (JAR). It is the ultimate load, which is the limit load multiplied with a prescribed factor of safety (usually 1.5). The limit load is defined as the maximum load to be expected in service. Generally speaking, the structure has to be able to support the ultimate load for at least 3 seconds [Ref 18]. It is very well possible that a component fails at a stress level considerably less than the stress level present when the ultimate load is applied. A component can fail due to fatigue whenever it is subjected to dynamic and fluctuating stresses [Ref 19].
Rotorcraft components in the rotor system are dynamically loaded. The main frequency at which these components are loaded is the rotor rotational frequency. A dynamic stress can be represented as in figure 12.

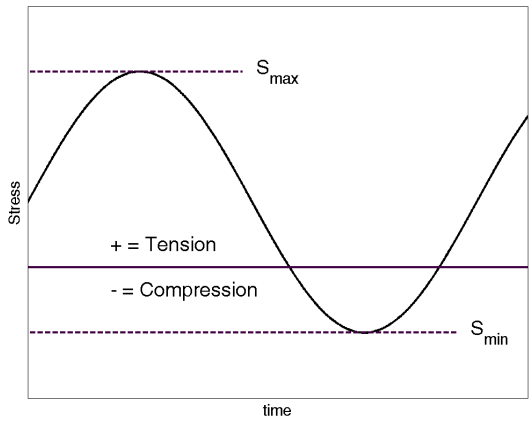

Figure 12: Dynamic loads

The sign convention is such that positive stresses are tensile. The maximum stress to be encountered in one cycle is called S_{max}, and the minimum stress is called S_{min}. The oscillatory stress S_a and the mean stress S_m can then simply be calculated with the following two formulas.

$$S_a = \frac{S_{\max} - S_{\min}}{2} \qquad (2)$$

$$S_m = \frac{S_{\max} + S_{\min}}{2} \qquad (3)$$

Exactly how many cycles will fail a component at a certain mean stress level and at a certain oscillatory load can be determined by laboratory tests. Results from these tests are usually summarised in a so-called S-N curve. From this curve one can read how many cycles at a certain oscillatory load, will fail the component. The mean stress level has an influence on this curve.

A typical S-N curve is given in figure 13.

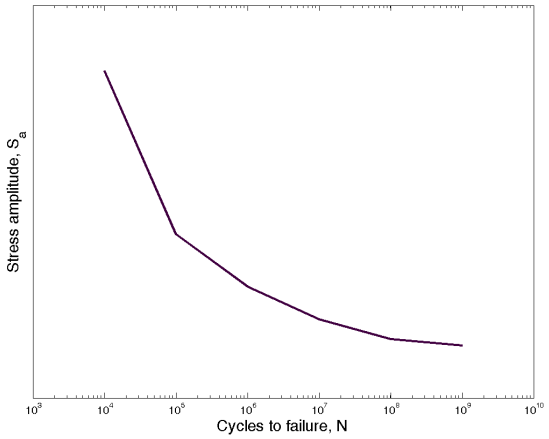

Figure 13: Example S-N curve

An increase in the mean stress will shift the curve up. The curve is generally split into two sections:

- Low cycle fatigue (< 10^4 – 10^5 cycles)
- High cycle fatigue (> 10^5 cycles)

For some materials, the S-N curve has a horizontal asymptote known as the fatigue limit or endurance limit. This limit is the stress below which a fatigue failure does not occur regardless of how many times the load is repeated. Aluminium does not have a fatigue limit that is clearly defined, so it is often taken as the stress at 5 * 10^8 cycles [Ref 20]. The other limit on the S-N curve will simply be the stress at which the component fails after 1 cycle, which is identical to the ultimate load.
Helicopter dynamic components can be designed with different methods with respect to the fatigue life. The most widely used methods are the safe-life method and the damage tolerance method. Other methods in use are e.g. the flaw-tolerance and fault tolerance method [Ref 21], which are derivatives of the safe-life and damage tolerance method.
The Safe life method works as follows. The oscillatory loads are measured in flight. They are subsequently compared with the appropriate S-N curves. The fatigue life can then be calculated with Miner's rule [Ref 23], using the flight stresses and the certification spectrum of the aircraft [Ref 22]. Miner's rule is a fairly simple but very effective rule. If S_a and S_m are known for one cycle, one can calculate the damage D due to one cycle with the S-N curve.

$$D = \frac{1}{N_i} \tag{4}$$

N_i is the number of cycles at which the component fails for the oscillatory load S_a and the mean stress S_m. The total damage is the sum of all the damage done by all the cycles in the certification spectrum. The component will fail when the damage has accumulated to 1. The component will have to be replaced before the safe life has been reached [Ref 22]. A margin of safety (three standard deviations from the mean) is usually applied to the S-N curve for this method [Ref 21].
The damage tolerance approach on the other hand assumes that there is already a crack present in the component. The time that it takes for this assumed crack to grow to a length where the component will fail is calculated with crack growth data of the component and with the loads that will be encountered in the flight certification spectrum of the aircraft. This time interval is called the crack growth life. Inspections of the component will be done frequently enough, based on the crack growth life, to find cracks before they can grow to their critical length [ref. 22].

Most rotorcraft components are designed with the safe life method because it is a very simple and effective method.
One of the goals of this study is to define a structural load severity scale, which can be used just like the well-known ADS-33 handling qualities requirements. The following scale is proposed, based on the literature survey described above:

Level 1: Stress level < Fatigue limit
Level 2: High Cycle fatigue loading
Level 3: Low Cycle fatigue loading
Level 4: Stress level > Ultimate load

The question remains now, how to transfer this scale to a metric for offline analysis and to a tool for evaluating mission task elements (MTE). One possible approach for evaluating MTE damage might be the following; the damage done to a component, during the MTE can be calculated with Miner's rule. The damage for the borders between the levels for any MTE can also be calculated with Miner's rule:

$$D_{23} = \frac{1}{N_{23}} \frac{2\pi}{\Omega} t_{MTE} \tag{5}$$

Where D_{23} is the damage on the border of level 2 and level 3, N_{23} is the number of cycles at which the component fails at the stress level on the border of level 2 and 3, and t_{MTE} is the time required for an MTE when it is performed exactly according to the definition in ADS-33. Similar formulas can be derived for the other two borders.

Mission Task Elements:

Level 1: $D_{MTE} < D_{12}$
Level 2: $D_{12} < D_{MTE} < D_{23}$
Level 3: $D_{23} < D_{MTE} < D_{34}$
Level 4: $D_{MTE} > D_{34}$

Unfortunately S-N curves are not always available. Also, one might want to use these scales while still in the design phase of the helicopter when exact dimensions of components are not yet determined or materials are not yet selected. Or one may want to use a load severity scale for more general structural loads such as hub loads. In these cases it is not possible to use the severity scales defined above. The so-called Load Amplification Factor (LAF) is therefore proposed. The LAF is simply the factor with which the steady state oscillatory load at the beginning of a manoeuvre is multiplied during the manoeuvre.

$$LAF = \frac{S_{a,\max}}{S_{a,ss}} \tag{6}$$

At the present moment, no S-N curves are available for the pitch link of the FGR.
Pavel and Padfield [Ref 24] have proposed a structural load metric in combination with a handling qualities metric that can be used for high-speed longitudinal manoeuvres with rotorcraft. They are called the agility quickness and the vibratory load quickness

$$Q_\gamma \triangleq \frac{n_{z,qs}^{pk}}{\Delta\gamma} \approx \frac{\dot{\gamma}}{\Delta\gamma} \tag{7}$$

$$Q_l \triangleq \frac{n_{z,pk}^{vib}}{\Delta\gamma} \tag{8}$$

At high speed, pilots are more interested in controlling the flight path angle than pitch attitude for most tasks. This is why the well-known pitch attitude quickness has been changed into flight path angle quickness (equation 7). The focus in this paper will be on the load quickness parameter because we are primarily interested in whether the structural loads can be reduced. The variable $n_{z,pk}^{vib}$ in the load quickness definition represents the peak amplitude in 'g units' in the vibratory components of the hub shears. This load quickness parameter was used to evaluate the vibratory loads of the FGR for pull-up manoeuvres. It is proposed here to slightly alter the definition of the load quickness parameter to make it applicable to the other load alleviation problem. So two definitions are proposed.

$$Q_{l,\gamma} = \frac{F_{pk}}{\Delta\gamma},\ Q_{l,\theta} = \frac{F_{pk}}{\Delta\theta} \tag{9}$$

One can be used in combination with the attitude quickness and one with agility quickness. F_{pk} in these formulas is the peak oscillatory load during a manoeuvre. After evaluation of the two load quickness definitions, conclusions can be drawn upon the advantages and shortcomings of these parameters.

In order to be able to use the load quickness as a design parameter, different structural load levels should be devised. The Load Amplification Factor (LAF) as explained before, can be used for this. Load Amplification Factor lines can be calculated by combining equations 6 and 9.

$$Q_{l,\gamma} = \frac{F_{ss}}{\Delta\gamma} LAF \tag{10}$$

Four Load Amplification Factor lines are shown in Fig. 14. The steady state peak oscillatory load is assumed to be equal to 1 in this case.

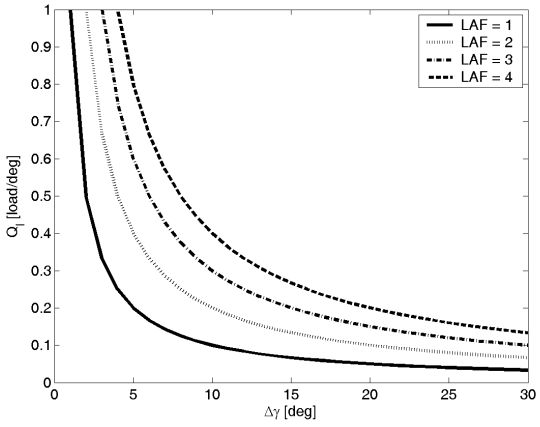

Figure 14: Load amplification factor lines

These lines have a similar shape as the well-known handling qualities levels for attitude quickness. The load quickness parameter in combination with the LAF will be used in the next paragraph to evaluate the controller.

4.3 Analysis of the SLA controller

The following four figures present the load quickness for SLA on and off, plotted against pitch attitude and flight path angle. The pitch link load is close to the steady state value (LAF=1) for control inputs up until 15% when the SLA controller is off. A significant increase can be seen when the control input is 20% (LAF≈2.5). It does not really make a difference whether the load quickness is plotted against flight path angle or pitch attitude when SLA is off. The loads are significantly reduced with the SLA controller on (LAF<2 in all cases). A larger control input is needed to achieve the same pitch attitude. However the load quickness plotted against flight path angle reveals an important result. The load is reduced significantly but the maximum achievable flight path angle is limited to approximately 15 degrees. At high speed, pilots are more interested in controlling flight path angle than pitch attitude. So in combination with these results, it is recommended to plot load quickness against flight path angle. Very important to note is that the transient loads reduction achieved with the linear model and the Coleman transformed pitch link loads is also achieved on the non-linear model.

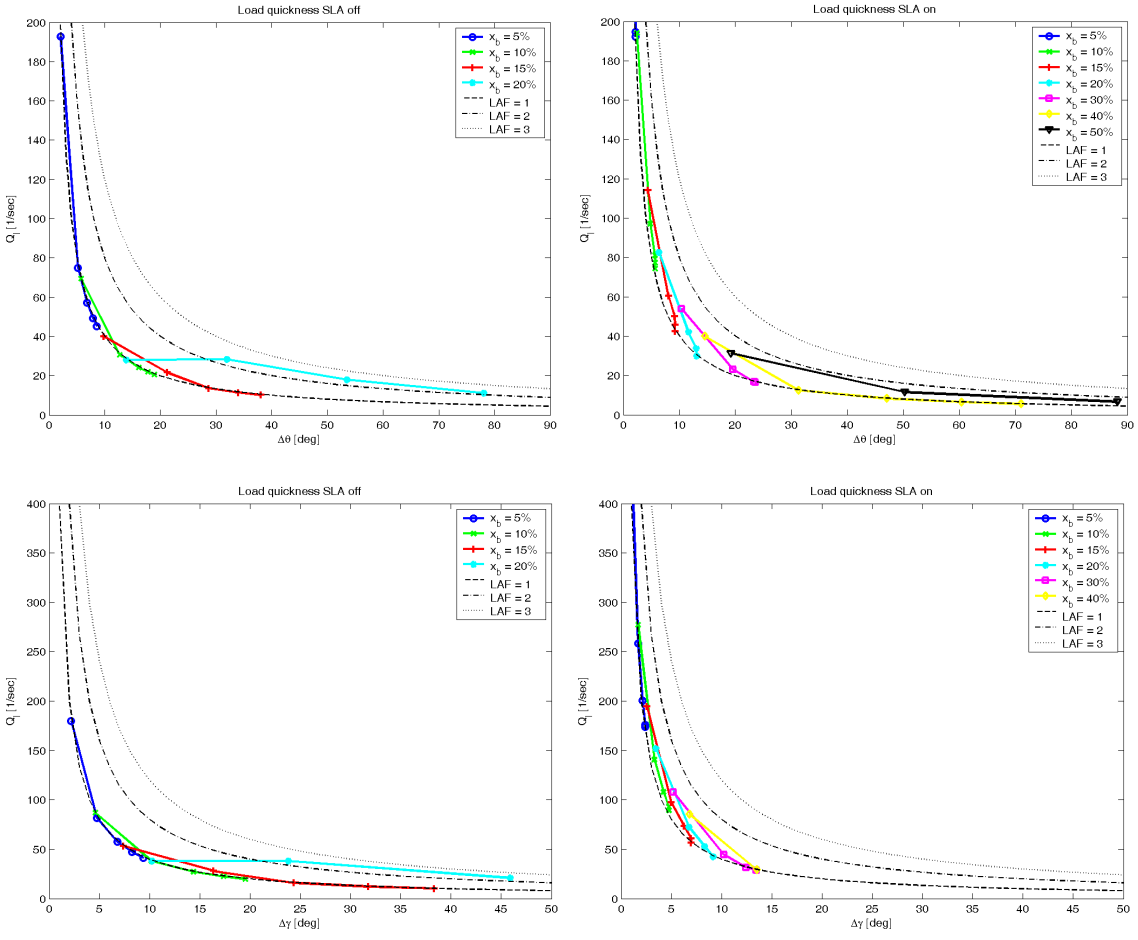

Figure 15: Load quickness plots

5. Conclusions and Recommendations

The present paper presents the preliminary design of an active controller for the FGR simulation model that reduces the pitch link loads for longitudinal manoeuvres at high speed. The paper also presents the development of a new structural load severity scale and shows how to apply the structural load quickness metric [Ref 24] to the evaluation of pitch link loads.

The FGR simulation model is expanded with a flexible pitch link model and a dynamic stall model to improve the model fidelity. Several

conclusions can be drawn from the impact of these models on the loads and flight mechanics prediction of the FGR. The dynamic stall model does not have a significant effect on the flight mechanics. It does have a significant effect on the magnitude of the pitch link load. The overall shape of the pitch link load as a function of azimuth remains similar, but the magnitude is about 40% lower. The flexible pitch link model on the other hand does not have a significant effect on the prediction of the pitch link load in steady state flight. The magnitude of the oscillatory pitch link load increases by approximately 10% whilst performing pull-up manoeuvres. Flight mechanics in pitch, roll and yaw are affected by only a couple of percent due to the introduction of the flexible pitch link, which was an expected result. The response due to a collective input is affected more however. The initial response due to a collective input is identical, but the achieved climb rate after the initial response is reduced.

Flight test data is absent unfortunately, so no clear conclusions can be made to determine whether these models really improve the fidelity. Future research will be conducted with a Flightlab model of the Bell 412 ASRA [Ref 6]. Flight test data will be available for this aircraft so it is a recommendation for further work to determine the fidelity improvements of the flexible pitch link and dynamic stall model.

An investigation of the pitch link loads showed that the steady state oscillatory pitch link loads increase significantly from a flight speed of 60 knots. The pitch link loads are amplified by a factor of 2.5 when executing high-speed pull up manoeuvres of about 2 'g'.

An H_∞ controller has been designed for high-speed longitudinal manoeuvres to reduce the pitch link loads. A Coleman transformation was performed on the pitch link loads in the non-linear simulation model to obtain a pitch link load envelope in the linear model that was used for control law design. The controller was designed first for the linear model and subsequently implemented on the non-linear model. The load quickness parameter [Ref 24] defined by Pavel and Padfield was altered slightly for the current problem because the original load quickness parameter was designed for vibratory hub loads and not for pitch link loads. A new structural load severity scale was also defined. With the use of this altered load quickness parameter and the new rating scale, it could be concluded that the pitch link loads can be reduced effectively. The new metrics appeared to be very useful for the evaluation of an SLA controller. It is a recommendation for further work to design this controller as a part of a complete flight control system for high-speed flight. A multi objective design between structural loads and handling qualities will then be done. This is where the new metrics will be most useful.

6. Acknowledgements

The research presented in this paper is funded by the U.K. Engineering and Physical Sciences Research Council through Research Grant GR/S42354/01.

7. References

1. Curtiss, H. C., Carson, F., Hill, J., Quackenbush, T., "Technical Note – Performance of a Sikorsky S-61 with a new main rotor," Journal of the American Helicopter Society, July 2003.
2. Kufeld, R. M., Bousman, W. G., "High load conditions measured on a UH-60A in maneuvering flight," 51st annual forum of the American Helicopter Society, Fort Worth, Texas, United States, May 1995.
3. Cresap, W. L., Myers, A. W., Viswanathan, S. P., "Design and development tests of a four-bladed light helicopter rotor system," 34th annual forum of the American Helicopter Society, May 1978.
4. Cresap, W. L., Myers, A. W., "Design and development of the model 412 helicopter," 36th annual forum of the American Helicopter Society, Washington D.C., United States, May 1980.
5. Yen, J. G., Weller, W. H., "Analysis and application of compliant rotor technology," 6th European Rotorcraft and Powered Lift Aircraft Forum, Bristol, England, September 1980.
6. Manimala, B., "Rotorcraft Simulation Modelling and Validation for Control Design and Load Prediction," 31st European Rotorcraft Forum, Florence, Italy, 2005.
7. Yen, J. G., Yuce, M., "Calculations of Pitch Link Loads in deep stall using state-of-the-art technology,"
8. Leishman, J. G., "Principles of Helicopter Aerodynamics," Cambridge

Aerospace Series, Cabridge, United Kingdom, 2000.
9. Johnson, W., “The response and airloading of helicopter rotor blades due to dynamic stall,” ASRL-TR 130-1, Massachusetts Institute of technology aeroelastic and structures research Laboratory, Cambridge, Massachusetts, May 1970.
10. Milgram, J., Chopra, I., Kottapalli, S., “Dynamically Tuned Blade Pitch Links for Vibration Reduction,” 50th annual forum of the American Helicopter Society, Washington DC, United States, May 1994.
11. Padfield, G. D., “Helicopter Flight Dynamics,” Blackwell Science, Oxford, United Kingdom, 1996.
12. Petot, D., “Differential Equation Modelling of Dynamic Stall,” La Recherche Aerospatiale. (5), 1989, pp. 59-72.
13. Johnson, W., “Rotorcraft Aerodynamics models for a comprehensive analysis,” 54th AHS annual forum, Washington DC, United States, May 1998.
14. Cheng-Jian He, Ronald Du Val, “An unsteady Airload Model with Dynamic Stall for Rotorcraft Simulation”, 50th annual forum of the American Helicopter Society, Washington DC, United States, May 1994.
15. Curtiss, H. C., Carson, F., Hill, J., Quackenbush,T., "Technical Note - Performance of a Sikorsky S-61 with a new main rotor", Revised version of 28th European Rotorcraft forum paper'
16. Manimala, B., Padfield, G. D., Walker, D., Naddei, M., Verde, L., Ciniglio, U., Rollet, P., Sandri, F., “Load alleviation in tilt rotor aircraft through active control: modelling and control concepts,” The Aeronautical Journal, Volume 108, Number 1082, pp. 175, April 2004.
17. Gahinet, P., Nemirovski, A., Laub, A. J., Chilali, M., “LMI Control Toolbox, for use with MATLAB®,” The Math Works Inc., Natick, Massachusetts, United States, 1995.
18. www.faa.gov
19. Callister, W. D., “Materials Science and Engineering an Introduction,” John Wiley & sons inc., 1997
20. Gere, J. M., Timoshenko, S. P., “Mechanics of Materials,” Chapman & Hall, London, United Kingdom, 1987.
21. Forth, S. C., Everett, R. A., Newman, J. A., “A novel approach to rotorcraft damage tolerance,” 6th Joint FAA/DoD/NASA aging aircraft conference, United States, September 2002.
22. Micheal, J., Collingwood, G., Augustine, M., Cronkhite, J., “Continued evaluation and spectrum development of a health and usage monitoring system,” DOT/FAA/AR-04/6, Ft. Worth, Texas, May 2004.
23. Miner, M. A., “Cumulative Damage in Fatigue,” ASME Journal of applied mechanics, Vol. 12, pp. PA159-164, 1945.
24. Pavel, M. D., Padfield, G. D., “Defining consistent ADS-33 metrics for agility enhancement and structural loads alleviation,” 58th AHS annual forum, Montreal, Canada, June 2002

Appendix A: Control system stiffness

One can derive the pitch link stiffness from the control system stiffness with figure A.1:

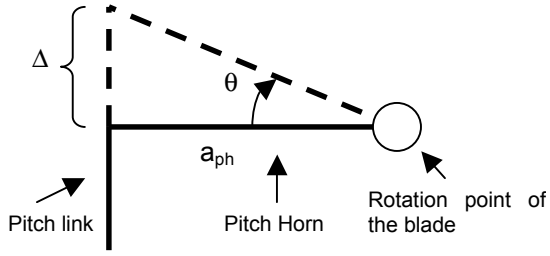

Figure A.1: Control system stiffness

The elongation of the pitch link follows from the geometry in figure A.1. The angle θ is assumed to be small and the pitch horn is assumed to be rigid.

$$\Delta = a_{ph} \sin\theta \approx a_{ph}\theta \qquad \text{(A.1)}$$

The force *F* needed to lengthen the pitch link is simply the pitch link stiffness $K_{pitchlink}$ multiplied with the elongation Δ. This force then creates a moment *M* at the rotation point of the blade.

$$F = K_{pitchlink}\Delta \qquad \text{(A.2)}$$

$$M = Fa_{ph} = K_{pitchlink}a_{ph}^2\theta \qquad \text{(A.3)}$$

This moment should equal the control system stiffness multiplied with the rotation angle θ.

$$M = k_\theta\theta \qquad \text{(A.4)}$$

Combining equations A.3 and A.4 then gives an equation, which can be used to calculate the pitch link stiffness from the data in table 3.1.

$$K_{pitchlink} = \frac{k_\theta}{a_{ph}^2} \qquad \text{(A.5)}$$

Appendix B: General control configuration

The general way to represent the controller (K) and the plant (P) for H_∞ design is shown in Figure B.1 [Ref 17].

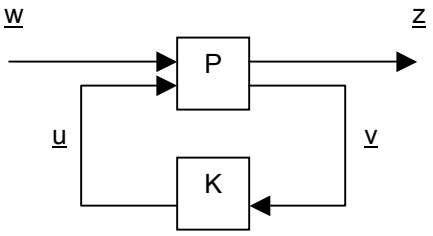

Figure B.1: General control configuration

w is the vector of reference signals, z is the vector of 'error' signals, v is the vector of feedback variables and u is the vector of control variables.